

Physics-Grounded Attached Shadow Detection Using Approximate 3D Geometry and Light Direction

Shilin Hu¹, Jingyi Xu¹, Sagnik Das¹, Dimitris Samaras^{1,†}, Hieu Le^{2,†}

¹Stony Brook University ²UNC Charlotte [†]Equal Advising

{shilhu, jingyixu, sadas, samaras}@cs.stonybrook.edu hle40@charlotte.edu

Abstract

Attached shadows occur on the surface of the occluder where light cannot reach because of self-occlusion. They are crucial for defining the three-dimensional structure of objects and enhancing scene understanding. Yet existing shadow detection methods mainly target cast shadows, and there are no dedicated datasets or models for detecting attached shadows. To address this gap, we introduce a framework that jointly detects cast and attached shadows by reasoning about their mutual relationship with scene illumination and geometry. Our system consists of a shadow detection module that predicts both shadow types separately, and a light estimation module that infers the light direction from the detected shadows. The estimated light direction, combined with surface normals, allows us to derive a geometry-consistent partial map that identifies regions likely to be self-occluded. This partial map is then fed back to refine shadow predictions, forming a closed-loop reasoning process that iteratively improves both shadow segmentation and light estimation. In order to train our method, we have constructed a dataset of 1,458 images with separate annotations for cast and attached shadows, enabling training and quantitative evaluation of both. Experimental results demonstrate that this iterative geometry–illumination reasoning substantially improves the detection of attached shadows, with at least 33% BER reduction, while maintaining strong full and cast shadow performance.

1. Introduction

Shadows define how we perceive shape, depth, and lighting in the world. They fall into two types: cast shadows, which appear on external surfaces and reveal spatial relations between objects [20, 33, 37, 48], and attached shadows, which form directly on an object’s surface where light is obstructed, exposing its geometry and orientation [18, 74]. Together, these two shadow types encode complementary cues about scene structure and illumination, enriching visual re-

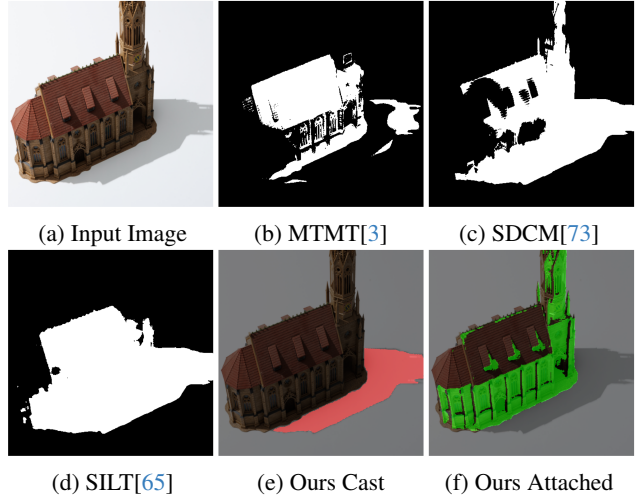


Figure 1. Existing shadow detection methods primarily focus on cast shadow detection and do not differentiate between cast and attached shadow types (b, c, d). In contrast, our method accurately segments both cast and attached shadows, separately (e, f).

alism and 3D perception [5, 31, 45, 49, 57, 68].

Despite their importance, recent shadow detection research has largely focused on cast shadows, mainly due to the lack of annotations and benchmarks for attached shadows [4, 16, 52–54, 65] (see Tab. 1). Furthermore, cast and attached shadows differ in nature and cannot be handled by the same detection strategy. Cast shadows typically form continuous regions that trace the outer contours of occluding objects, while attached shadows are often fragmented, appearing on the object’s own surface where local geometry turns away from the light. The appearance of attached shadows is therefore governed by fine surface orientation and material variations rather than global shape boundaries, making attached shadow detection a fundamentally different and more geometry-dependent problem.

To bridge this gap, we introduce a framework that jointly detects cast and attached shadows by explicitly modeling their dependence on light direction and surface geometry.

Table 1. **Comparison of shadow detection datasets.** Only our dataset annotates the attached shadow explicitly.

Dataset	Attached	#Imgs	Cast/Att. Split
SBU [52]	✓(occasional)	4.1K	✗
ISTD [53]	✗	1.9K	✗
SOBA [54]	✗	1.0K	✗
ViSha [4]	✗	11.7K	✗
SILT [65]	✓	0.6K	✗
CUHK [16]	✓	10.5K	✗
Ours	✓	1.5K	✓

The core idea is straightforward: surface regions that face away from the light are expected to be in shadow. With a known light direction and reliable surface normals [66], attached shadows can be directly inferred; when lighting is unknown, cast and attached shadows provide strong cues to recover it. We exploit this reciprocal relationship between light estimation and shadow formation to form a closed feedback loop, in which each component iteratively refines the other. This physically grounded formulation unifies classical illumination reasoning [9, 12, 37, 41, 44] with modern deep shadow detection.

Accordingly, we propose a dual-module architecture consisting of a *shadow detection* module and a *light estimation* module. The shadow detection module predicts both cast and attached shadows, while the light estimation module infers the light direction using detected shadows and surface normals as input. The estimated light direction is then used to compute a partial attached shadow map, which serves as an additional input to refine shadow detection. These two modules form a closed-loop system that operates iteratively. During inference, we run multiple passes on the same input image, progressively refining both shadow detection and light estimation. With each pass, the newly detected shadows and updated light direction act as improved priors, enabling iterative refinement of cast shadows, attached shadows, and light estimation.

To enable training and evaluation on a unified benchmark for cast and attached shadows, we curate a dataset of 1,458 images—1,166 for training and 292 for testing—with manually annotated masks for cast and attached shadows, sourced from WSRD [50], SOBA [54], and CUHK [16] datasets. The dataset spans diverse scenes and includes carefully annotated attached shadow labels, addressing a key gap in existing resources and encouraging further research on shadow detection. Experimental results demonstrate that our design effectively leverages information from both modules to enhance shadow detection and light direction estimation through our iterative learning scheme, outperforming prior methods in separately detecting attached and cast shadows, as illustrated in Fig. 1.

To summarize, our contributions are as follows:

- A framework that enables the simultaneous detection of cast and attached shadows through joint learning with light estimation.
- An iterative training scheme that mutually incorporates lighting and shadow cues for shadow detection and light estimation, enhancing each other’s performance.
- A curated dataset with separate cast and attached shadow annotations, enabling both training and standardized evaluation of methods that detect each shadow type.

2. Related works

Shadow detection and removal [6, 11, 13, 15, 17, 21–23, 25, 29, 40] are fundamental tasks in computer vision, where accurate shadow handling is crucial for tasks such as scene understanding [24, 27, 28] and generation [59–64]. Earlier shadow detection studies [32–36, 42] extensively explored the relationship between lighting and shadows. Panagopoulos *et al.* [37] were the first to jointly model shadow detection and light estimation using coarse scene geometry. However, their approach relied on simplified geometry and idealized physical models, which limited its ability to handle the complexities and variations in real-world images.

Recent deep learning advancements have significantly improved shadow detection [2, 14, 16, 26, 53, 70, 71]. Ding *et al.* [8] introduced an attentive recurrent GAN that iteratively detects and removes shadows. Chen *et al.* [3] leveraged multiple cues from shadow regions, edges, and shadow counts, using a student-teacher model. Zhu *et al.* [72] noted that deep shadow detectors were overly reliant on intensity cues and proposed a feature decomposition and re-weighting approach to reduce intensity bias. SDCM [73] used a complementary mechanism to jointly detect shadow and non-shadow regions by transferring deactivated intermediate features between branches. Sun *et al.* [47] focused on preserving multi-scale contrast information by mapping RAW images to sRGB representations of varying intensities. More recently, SwinShadow [58] leveraged a transformer-based architecture with a shifted window mechanism to better detect adjacent shadows by capturing hierarchical contextual details. In addition, several approaches have targeted more specialized tasks. [54–56] focused on the instance shadow detection task, concentrating on cast shadows associated with annotated objects.

While these recent methods have significantly advanced shadow detection, they do not explicitly address the unique challenge of detecting attached shadows. Several methods and datasets acknowledge the importance of attached shadows. Yang *et al.* [65] annotated attached shadows for the SBU-test set and proposed a method that aggressively accepts predicted shadows as the new ground truth during training. Hu *et al.* [16] introduced a benchmark in which a

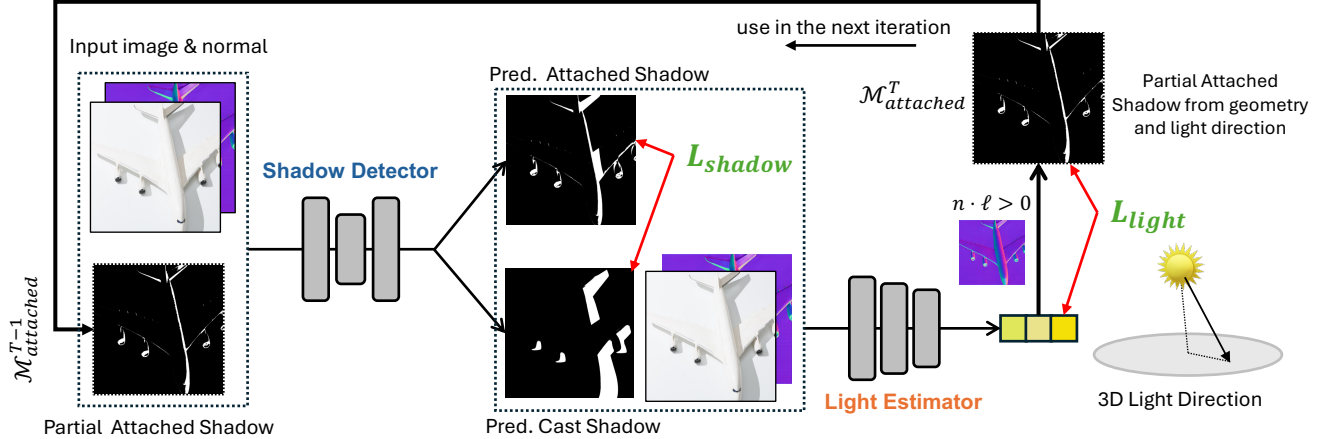


Figure 2. **Overview.** Our network consists of two modules: a shadow detection module and a light estimation module. The shadow detection module simultaneously predicts both cast and attached shadows, while the light estimation module predicts a three-dimensional light direction and generates a partial attached shadow map from the estimated light direction. This partial map is then fed back into the shadow detection module as an additional input during iterative training.

large portion of the shadows are attached shadows. However, these approaches still treat cast and attached shadows uniformly, ignoring their distinctions.

Estimated lighting has been widely used in computer vision tasks. Existing illumination representations can be broadly categorized into three types: environment maps [43, 51], light probes [1, 39], and parameterized lighting models [7, 67]. In this paper, we adopt the three-dimensional light-direction parameterization from [10].

3. Method

Our framework detects both cast and attached shadows by jointly learning shadow detection and light estimation using a single image and its corresponding normal map, as shown in Fig. 2. Using the estimated light direction and surface normals, we generate a geometry-derived partial attached shadow map based on the physics of shadow formation. This map is then incorporated as an additional input to refine shadow detection. Similarly, detected shadows serve as an auxiliary input for light estimation. The two modules operate in a closed loop, iteratively refining their outputs over multiple forward passes, improving both shadow detection and light estimation.

3.1. Problem Setup

Attached shadows form due to the interaction between surface orientation and light direction, typically occurring on surfaces oriented away from the light source. In this paper, we define attached shadows as those appearing on the object itself, while cast shadows are those projected onto external surfaces, as illustrated in Fig. 3. We assume a single scene-wide directional light shared across the image, and define ℓ to point from the light toward the scene.



Figure 3. **Problem Setup.** The goal is to separately predict cast and attached shadows. Cast shadows appear on external surfaces, while attached shadows form directly on the object itself.

3.2. Framework Overview

As illustrated in Fig. 2, our framework consists of two primary modules: a shadow detection module and a light estimation module. The shadow detection module is formulated as a multi-class segmentation task over $\{\text{bg}, \text{cast}, \text{attached}\}$, taking the RGB image and its corresponding normal map as input. Meanwhile, the light estimation module leverages the normal map and the predicted shadows to estimate the light direction, represented as a three-dimensional vector. By integrating these modules within a unified framework, our approach enables mutual reinforcement between shadow detection and light estimation, thereby improving overall performance.

3.2.1. Iterative Training

Shadow and illumination serve as mutual cues for estimating each other [37]. Similarly, our framework jointly and iteratively refines shadow detection and light estimation.

Each training step consists of multiple iterations. In each iteration, we use the predicted light direction and surface normals to generate a *partial attached shadow map* derived from geometry and light direction. This map iden-

tifies pixels that are likely to belong to attached shadows based purely on the object’s surface normals and the light direction. It is not a complete attached shadow mask because it does not model visibility or geometric blocking, so it cannot capture cases where one surface region blocks light from reaching another. Still, it provides reliable local cues near contact regions and boundaries and is then fed to the shadow detection module in the next iteration as an additional input to predict the complete attached and cast shadow masks.

Specifically, given a light direction vector $\ell \in \mathbb{R}^3$ pointing from the light source toward the surface, and the surface normals $\mathbf{n} \in \mathbb{R}^{H \times W \times 3}$, the partial attached shadow map, denoted as $\mathcal{M}_{\text{attached}}$, includes surface points facing away from the light source as:

$$\mathcal{M}_{\text{attached}} = \begin{cases} 1, & \mathbf{n} \cdot \ell > 0 \\ 0, & \mathbf{n} \cdot \ell \leq 0 \end{cases} \quad (1)$$

This geometry-based map serves as an initial physical constraint. As the estimated light direction becomes more accurate across iterations, the map is progressively refined, leading to improved shadow detection and, in turn, better light estimation. In the first iteration, the shadow detection module is initialized with an all-ones map.

3.2.2. Training Objectives

We jointly optimize the two modules by a complementary objective for shadow detection and light estimation. The shadow loss enforces accurate and well-separated segmentation of cast and attached shadows, while the light loss constrains illumination estimation and its physical consistency. Together, these objectives encourage stable convergence of the iterative refinement process described above.

Shadow Detection Loss. We supervise the shadow detector at two complementary levels. First, for global shadow segmentation (shadow vs. background), we sum subclass logits with the log-sum-exp (LSE), $\text{LSE}(a, b) = \log(e^a + e^b)$. Let $z_{\text{bg}}, z_{\text{cast}}, z_{\text{att}} \in \mathbb{R}$ be per-pixel logits, we define:

$$s = \text{LSE}(z_{\text{cast}}, z_{\text{att}}) - z_{\text{bg}}, \quad (2)$$

We then match s to the union ground-truth shadow mask $y_{\text{union}} \in \{0, 1\}$ using a binary cross-entropy (BCE) term plus a Dice [46] regularizer:

$$\mathcal{L}_{\text{seg}} = \text{BCE}(s, y_{\text{union}}) + \lambda_{\text{Dice}} \text{Dice}(s, y_{\text{union}}), \quad (3)$$

Second, to distinguish shadow types (cast vs. attached), we apply a standard multi-class cross-entropy (CE) on the full logits with per-pixel labels $y_{\text{type}} \in \{\text{bg, cast, att}\}$. In addition, we impose a class-conditional margin on the cast vs. attached logits to sharpen their separation. Let $d^{(i)} = z_{\text{cast}}^{(i)} - z_{\text{att}}^{(i)}$, and let Ω_{cast} and Ω_{att} be the index sets of pixels labeled cast and attached, respectively. With margin

$m = 0.2$, we have:

$$\begin{aligned} \mathcal{L}_{\text{dist}} &= \frac{1}{|\Omega_{\text{cast}}|} \sum_{i \in \Omega_{\text{cast}}} \max(0, m - d^{(i)}) \\ &+ \frac{1}{|\Omega_{\text{att}}|} \sum_{i \in \Omega_{\text{att}}} \max(0, m + d^{(i)}), \end{aligned} \quad (4)$$

$$\mathcal{L}_{\text{type}} = \text{CE}(\mathbf{z}, y_{\text{type}}) + \lambda_{\text{dist}} \mathcal{L}_{\text{dist}}, \quad (5)$$

Together, this supervision encourages robust recovery of overall shadow extent while explicitly teaching the model to separate attached from cast shadows. The total shadow loss is therefore:

$$\mathcal{L}_{\text{shadow}} = \mathcal{L}_{\text{seg}} + \mathcal{L}_{\text{type}}, \quad (6)$$

Light Estimation Loss. We constrain the light estimator with three complementary losses. First, we encourage light cues to localize attached shadows by aligning the $\mathcal{M}_{\text{attached}}$ to the ground truth attached shadow mask $y_{\text{att}} \in \{0, 1\}$ via a weighted BCE. Second, we regress the predicted light direction $\hat{\ell}$ to a heuristic target ℓ^* (from geometry; see Sec. 4) with an ℓ_1 loss. And third, we enforce a unit norm:

$$\mathcal{L}_{\text{att}} = \text{BCE}_w(\mathcal{M}_{\text{attached}}, y_{\text{att}}). \quad (7)$$

$$\mathcal{L}_{\text{dir}} = \|\hat{\ell} - \ell^*\|_1, \quad (8)$$

$$\mathcal{L}_{\text{unit}} = (\|\hat{\ell}\|_2 - 1)^2, \quad (9)$$

The overall light loss is then:

$$\mathcal{L}_{\text{light}} = \lambda_{\text{att}} \mathcal{L}_{\text{att}} + \lambda_{\text{dir}} \mathcal{L}_{\text{dir}} + \lambda_{\text{unit}} \mathcal{L}_{\text{unit}}, \quad (10)$$

Finally, the full training objective is:

$$\mathcal{L}_{\text{total}} = \mathcal{L}_{\text{shadow}} + \mathcal{L}_{\text{light}}. \quad (11)$$

4. Dataset

We introduce the first dataset specifically curated for cast and attached shadow detection, consisting of 1,166 training and 292 testing images, each paired with surface normal maps, 3D heuristic light directions, binary cast and attached masks, and an “undefined” shadow mask. Fig. 4 presents examples from our dataset. Our dataset is compiled from three public sources: 220 images from the WSRD dataset [50], which provides pairs of shadow and shadow-free images, 710 images from the SOBA dataset [54], which includes shadow images, and instance-level cast shadow masks, and 538 images from CUHK [16], which provides scene-level full-shadow masks.

Accurately annotating cast and attached shadows per pixel in natural scenes is highly labor-intensive due to the

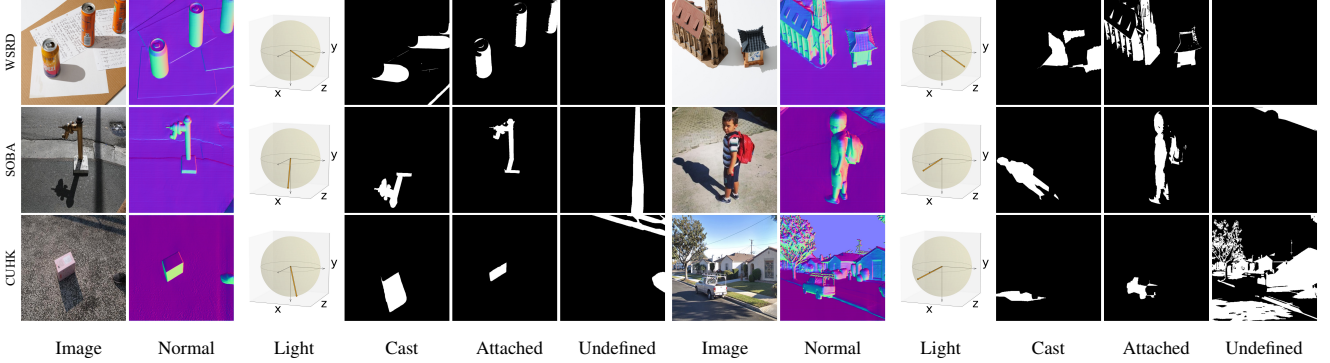


Figure 4. **Examples of our proposed dataset.** We curate the dataset from the WSRD [50], SOBA [54], and CUHK [16] datasets. Each image is paired with its corresponding normal map, light direction, cast shadow, attached shadow, and “undefined” shadow masks. The light direction is specified in a camera-centric frame, with $+x$ right, $+y$ down, and $+z$ inward.

complexity of mixed shadow types. To simplify this process, we restrict fine-grained annotation to foreground objects: we manually mark the cast and attached shadows produced by these objects. All remaining shadow pixels not attributable to the annotated foreground objects are labeled as *undefined shadows*. We use undefined shadows only for full-shadow supervision and evaluation, excluding them from both training and evaluation of cast/attached categories. This avoids bias from ambiguous ownership and yields a fairer assessment of shadow prediction performance. Additional details on data preparation are provided in the supplementary material.

Normal Maps. Since scene geometry is crucial for accurately identifying attached shadow regions, we use a recent foundation model [66] to generate relative depth maps, which are subsequently converted into normal maps.

Object Masks. Extracted using BiRefNet [69], these masks are used only for annotation and evaluation purposes.

Cast and Attached Shadow Masks. Utilizing the object masks, we manually annotate and correct the cast and attached shadow masks for SOBA and CUHK images. Since WSRD lacks shadow masks, we derive full-shadow masks using color-space subtraction between shadow and shadow-free images, then annotate cast and attached shadows.

Light Directions. WSRD images are captured under a well-calibrated, fixed-lighting system [50]; therefore we manually compute ground-truth 3D light directions. For SOBA and CUHK, we estimate a heuristic 3D direction as follows: (i) We compute a 2D image-plane direction by connecting the centroid of a foreground object to the centroid of its cast shadow. Under a directional-light assumption, a cast shadow is the object translated along the illumination direction and projected onto the receiving surface; hence, the displacement from object to shadow provides the illumination ray’s image-plane projection. (ii) We infer the third component using the relative depth between the object region and its cast shadow region. If the shadow lies on a surface deeper than the object, the illumination has a

component pointing “into” the scene; if it lies shallower, the component points “toward” the camera. Combining this signed component with the in-plane vector and normalizing yields a 3D unit direction in our camera-centric frame ($+x$ right, $+y$ down, and $+z$ inward).

5. Experiments & Results

Implementation Details. The proposed framework is implemented using PyTorch [38], with the shadow detection module adapted from SILT [65] and the light estimation module based on ConvNeXt-S [30]. We train our framework with the Adam [19] optimizer with a learning rate of 5×10^{-4} for 20 epochs, with a batch size of 4. We set the hyperparameters λ_{Dice} , λ_{dist} , λ_{att} , λ_{dir} and λ_{unit} to 0.1, 0.2, 0.4, 0.5, and 0.1, respectively. Further details and model modifications are provided in the supplementary material.

Evaluation Methods and Metrics. We conduct a comprehensive comparison of our method against seven state-of-the-art shadow detection approaches: BDRAR [71], DSD [70], FSDNet [16], MTMT [3], FDRNet [72], SDCM [73], and SILT [65]. All previous methods are evaluated using SBU pre-trained models. For BDRAR, FSDNet, FDRNet, and SILT, we further retrain them on our proposed dataset with supervision over the full shadow masks. Evaluations are conducted on our test set using standard metrics: $\text{Precision} = TP/(TP + FP)$, $\text{Recall} = TP/(TP + FN)$, and the F-measure $F = 2 \times \text{Precision} \times \text{Recall}/(\text{Precision} + \text{Recall})$. We also report the balanced error rate (BER), $\text{BER} = 100 \times (1 - \frac{1}{2} [TP/(TP + FN) + TN/(TN + FP)])$. Here, TP , TN , FP , and FN denote the numbers of true positives, true negatives, false positives, and false negatives, respectively. For previous shadow detection methods, object masks are used to separate predictions for cast and attached shadows. Cast shadow evaluation is performed by excluding the undefined shadow region. Attached shadow evaluation is limited to the object region. More results are provided in the supplementary material.

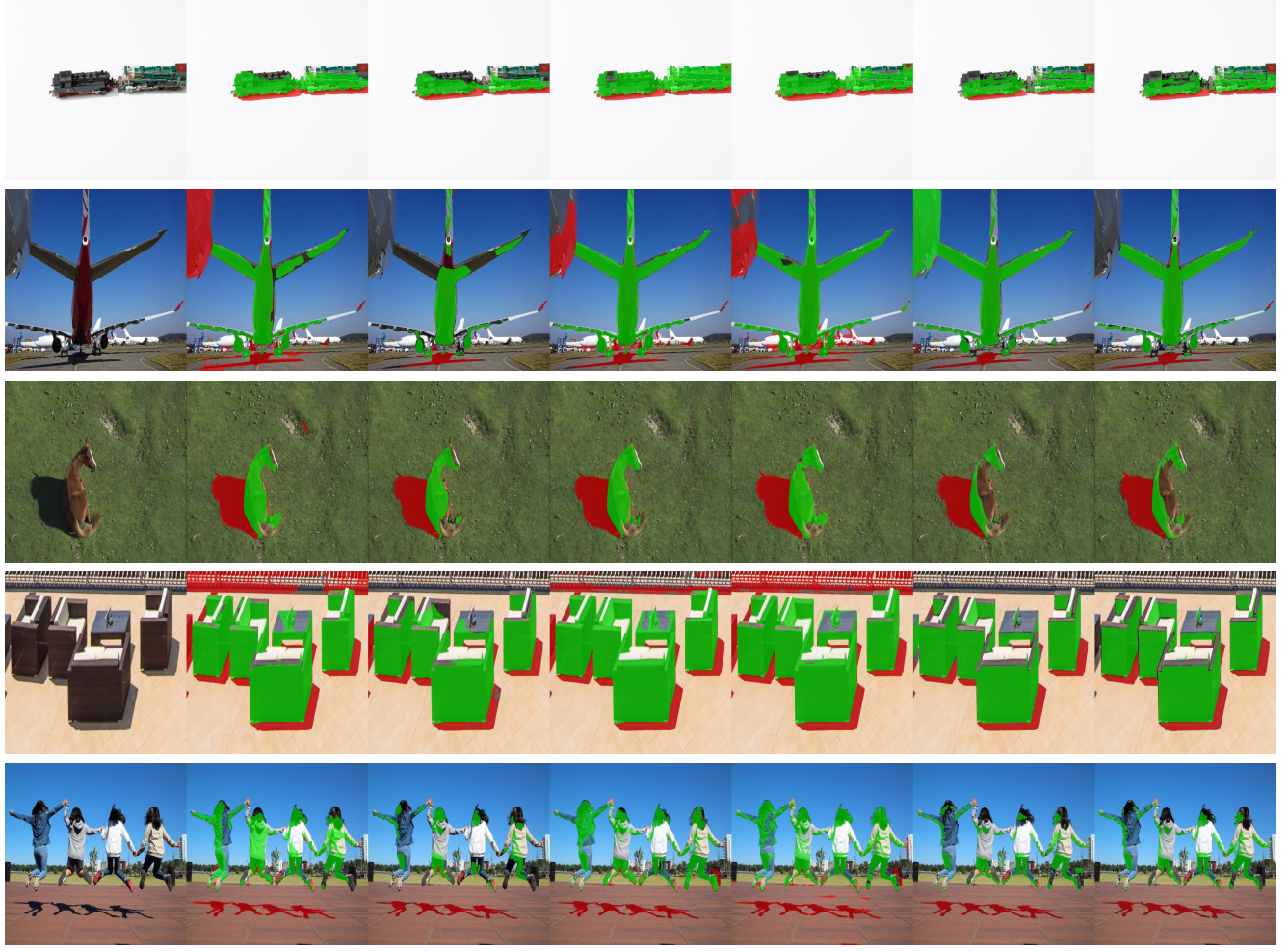


Image BDRAR[71]† FSDNet[16]† FDRNet[72]† SILT[65]† Ours GT

Figure 5. Qualitative comparison of the proposed framework for detecting cast and attached shadows against retrained BDRAR[71], FSDNet[16], FDRNet[72], and SILT[65] models on our dataset. Colored masks are overlaid on the original image (Green: Attached, Red: Cast). Our proposed physics-grounded iterative approach better captures attached shadows.

5.1. Comparison with SOTA methods

Quantitative Comparisons. Tab. 2 reports BER and F1 scores for full, cast, and attached shadows. Our method achieves the best performance on full and attached shadows in both metrics and the strongest cast F1, while its cast BER remains comparable to prior approaches. We first evaluate the SBU-pretrained baselines, which are cast-focused. All methods show a clear gap between cast and attached performance, with attached BER being worse by about 20–30 points. These models primarily capture cast shadows that usually appear as contiguous, lower-intensity regions, and only occasionally detect attached shadows when they resemble cast shadows in appearance. These results expose the limits of current cast-biased datasets and models in detecting attached shadows. We then retrain the baselines on our data using full-shadow supervision. This narrows the

gap but the baselines still struggle with attached shadows. A key limitation is that they treat the two shadow types uniformly and ignore that attached shadows are governed by surface orientation and contact rather than occlusion. In contrast, our method leverages geometry and lighting by using surface normals and estimating a light direction. These explicit physical cues let the model reason about where attached shadows should occur while preserving cast performance. As a result, attached shadow BER is substantially reduced by at least 33% relative to prior methods, while maintaining strong performance on full and cast shadows.

Qualitative Comparisons. Fig. 5 shows visual comparisons between our method and four baselines retrained on our dataset. The baselines produce a single shadow mask, so we use the object mask to split their outputs into attached and cast. Our method follows the occluder geometry

Table 2. Quantitative comparison of our method against state-of-the-art approaches on the proposed dataset. We report BER and F1 scores for full, cast, and attached shadows. Methods fine-tuned on our training set are marked with \dagger . The best results are in **bold**.

Methods	Full		Cast		Attached	
	BER \downarrow	F1 \uparrow	BER \downarrow	F1 \uparrow	BER \downarrow	F1 \uparrow
BDRAR[71]	21.29	70.53	7.23	79.64	35.41	53.32
DSD[70]	22.53	68.75	7.83	80.10	35.93	51.74
FSDNet[16]	24.46	66.09	10.51	79.16	37.53	46.24
MTMT[3]	33.10	50.00	15.16	74.66	42.02	38.10
FDRNet[72]	23.69	65.69	8.95	71.65	34.82	55.15
SDCM[73]	24.27	66.51	7.88	83.42	36.83	49.02
SILT[65]	20.20	71.51	4.64	80.39	32.70	60.23
BDRAR \dagger	8.15	83.95	5.18	72.86	20.75	82.69
FSDNet \dagger	10.17	85.10	5.82	81.94	19.49	80.57
FDRNet \dagger	8.62	83.00	4.65	73.27	23.11	81.42
SILT \dagger	6.51	82.98	4.52	68.31	26.57	80.72
Ours	6.50	86.61	5.04	85.46	12.93	86.49



Figure 6. Examples where only the foreground object is annotated, yet our method correctly predicts cast and attached shadows across the entire image.

and the estimated light direction: surfaces that face away from the light are labeled as attached shadows with clear, geometry-consistent boundaries (rows 1 and 2). In contrast, the baselines rely mainly on image appearance and tend to mark dark regions as shadows, even when those surfaces are actually lit (rows 3 and 4). By using surface normals, an estimated light direction, and separate predictions for cast and attached shadows, our method improves attached shadow quality while maintaining strong cast predictions. We further show qualitative results in Fig. 6 where the ground-truth annotations cover only foreground objects, yet our method correctly assigns cast and attached labels across the remaining undefined shadow regions. This ability reduces the need for dense annotation and supports scalable future learning via pseudo-labels or weak supervision.

Table 3. Ablation studies on the proposed physics-grounded framework. We report the BER and F1 score for full, cast and attached shadow detection.

Methods	Full		Cast		Attached	
	BER	F1	BER	F1	BER	F1
No Normal	7.60	85.46	7.82	79.33	20.87	77.07
Non-iterative	7.57	85.99	6.14	87.75	15.10	83.91
2 iterations	6.63	87.77	5.41	86.75	13.22	85.63
3 iterations (final)	6.50	86.61	5.04	85.46	12.92	86.49
5 iterations	6.11	87.14	5.83	85.57	13.51	85.74
No $\mathcal{L}_{\text{dist}}$	7.19	86.25	6.16	85.69	13.45	85.38
No \mathcal{L}_{att}	6.89	87.03	5.81	85.26	14.61	84.24
No \mathcal{L}_{dir}	7.50	86.42	4.97	85.02	15.26	83.59

5.2. Ablation Studies

To validate the effectiveness of our framework design, we conduct ablation studies to analyze the contributions of the surface normal guidance for geometry awareness, the proposed iterative learning scheme, and each loss component.

Effect of geometry guidance. We first examine the importance of incorporating surface normals as geometry guidance. Removing the use of surface normals reverts the framework to a simple multi-class segmentation model with class-specific labels. This removal noticeably degrades performance across all metrics, especially for attached shadows, yielding results comparable to retrained baselines. This finding confirms that surface normal information provides valuable spatial priors for accurate shadow separation.

Effect of iterative learning. We first evaluate our framework without iterative learning, where shadow detection and light estimation are jointly trained with normal maps but without feeding the partial attached shadow map back into the detector. As shown in Tab. 3, this non-iterative setting outperforms the variant without normal map guidance, confirming the benefit of geometry awareness. We then study the iterative training scheme by testing 2, 3, and 5 iterations. Introducing iterative feedback consistently enhances shadow prediction performance: two iterations yield the largest gains, and improvements plateau at three iterations. Fig. 7 illustrates the intermediate predictions of our final adopted 3-step setting. The second iteration brings clear visual improvements, while performance stabilizes at three iterations. Extending to five iterations slightly improves full-shadow accuracy but hurts class-specific results, likely due to over-refinement on the partial shadow map. Regarding efficiency, the computational cost increases roughly linearly with the number of iterations; our 3-step configuration requires about three times the processing time compared to the non-iterative baseline (0.18 s vs. 0.55 s). Overall, while geometry provides strong priors, iterative refinement further improves segmentation.

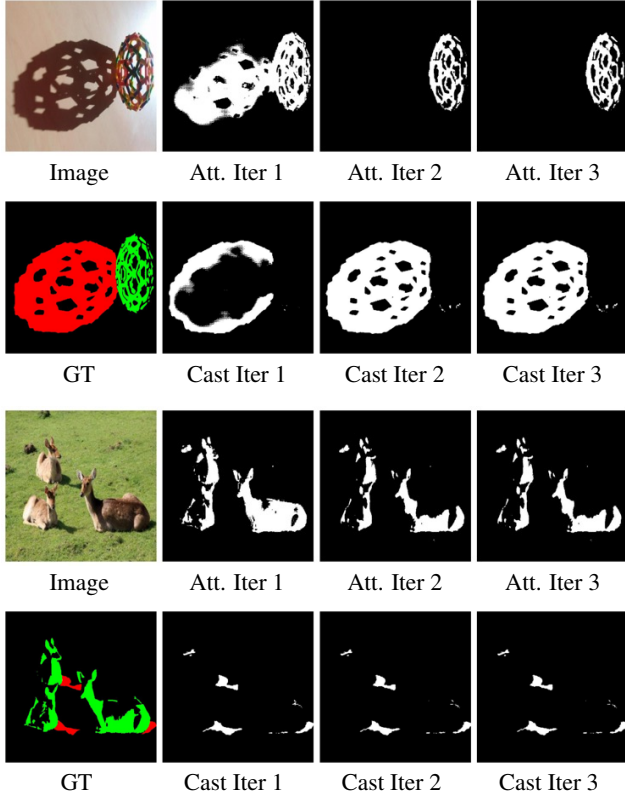


Figure 7. Effectiveness of the iterative learning scheme. Our proposed feedback mechanism progressively refines the shadow predictions, with clear visual improvements at the second iteration, and stabilizes at the third.

Effect of loss design. We further study the contribution of each loss component by ablating them individually during training. Excluding any single term leads to performance degradation, indicating that each loss plays a complementary role in guiding the network. The distance-based term $\mathcal{L}_{\text{dist}}$ regularizes the logits of cast and attached shadows through a class-conditional margin, enforcing a clearer decision boundary between the two categories. The light-related losses, \mathcal{L}_{att} and \mathcal{L}_{dir} , guide the light estimator to produce more accurate and spatially coherent partial maps by aligning its outputs with ground-truth cues and enforcing directional consistency. Together, these objectives promote robust geometry–light interaction and lead to more reliable shadow predictions.

6. Limitations

As an initial step toward detecting both cast and attached shadows, our framework has certain limitations. First, our framework relies on scene geometry derived from normal maps generated by an off-the-shelf model [66]. However, this foundation model does not always yield accurate surface orientations, as illustrated in Fig. 8 (first row). Although our method still performs reasonably, further im-

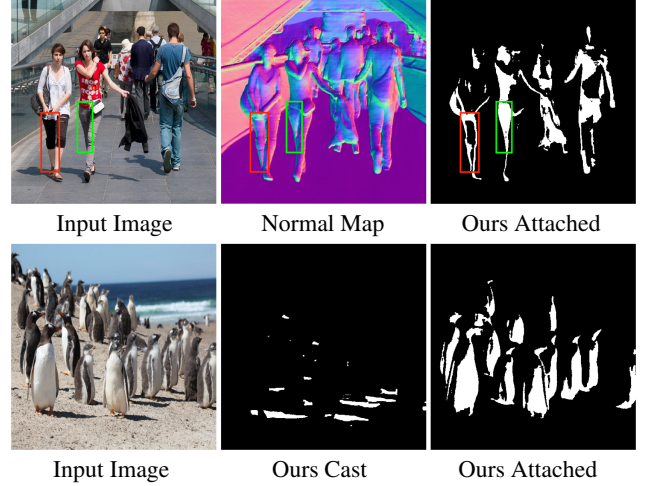


Figure 8. **Limitations.** The first row shows errors in attached shadow predictions due to an inaccurate normal map (compare highlighted regions). The second row illustrates detected shadow masks when multiple objects are present.

provements to foundation models could address this limitation by providing more reliable geometric information. Secondly, our method detects both cast and attached shadows but lacks a mechanism to explicitly associate each cast shadow with its corresponding attached shadow, as shown in Fig. 8 (second row) when multiple objects are present. This may limit downstream tasks such as instance-level shadow removal or object placement reasoning. Additionally, our approach assumes a single directional light source, which may not generalize well to complex multi-source lighting conditions, commonly found in indoor or night-time settings. Future work could integrate instance information to establish explicit cast-attached shadow pairings while increasing dataset diversity to enhance robustness across varied lighting environments.

7. Conclusion

We propose a framework for the separate detection of cast and attached shadows, addressing a key gap in current shadow detection research. Unlike previous methods that focused mainly on cast shadows, our approach leverages light direction, surface geometry, and shadow formation to detect the two shadow types simultaneously. Our dual-module architecture, featuring an iterative feedback loop between shadow detection and light estimation, enhances the accuracy and robustness of attached shadow detection. Experiments show that our framework outperforms prior methods in detecting both shadow types, underscoring the value of integrating lighting cues and geometric information. We introduce a new dataset for attached shadow detection with high-quality annotations of cast and attached shadows, to support future research and model development.

References

[1] Jiayang Bai, Zhen He, Shan Yang, Jie Guo, Zhenyu Chen, Yan Zhang, and Yanwen Guo. Local-to-global panorama inpainting for locale-aware indoor lighting prediction. *IEEE Transactions on Visualization and Computer Graphics*, 29(11):4405–4416, 2023. 3

[2] Tianrun Chen, Lanyun Zhu, Chaotao Deng, Runlong Cao, Yan Wang, Shangzhan Zhang, Zejian Li, Lingyun Sun, Ying Zang, and Papa Mao. Sam-adapter: Adapting segment anything in underperformed scenes. In *Proceedings of the IEEE/CVF International Conference on Computer Vision*, pages 3367–3375, 2023. 2

[3] Zhihao Chen, Lei Zhu, Liang Wan, Song Wang, Wei Feng, and Pheng-Ann Heng. A multi-task mean teacher for semi-supervised shadow detection. In *Proceedings of the IEEE/CVF Conference on computer vision and pattern recognition*, pages 5611–5620, 2020. 1, 2, 5, 7

[4] Zhihao Chen, Liang Wan, Lei Zhu, Jia Shen, Huazhu Fu, Wennan Liu, and Jing Qin. Triple-cooperative video shadow detection. In *Proceedings of the IEEE/CVF Conference on Computer Vision and Pattern Recognition*, pages 2715–2724, 2021. 1, 2

[5] Yung-Yu Chuang, Dan B Goldman, Brian Curless, David H. Salesin, and Richard Szeliski. Shadow matting and compositing. *ACM Transactions on Graphics*, 22(3):494–500, 2003. Sepcial Issue of the SIGGRAPH 2003 Proceedings. 1

[6] Xiaodong Cun, Chi-Man Pun, and Cheng Shi. Towards ghost-free shadow removal via dual hierarchical aggregation network and shadow matting gan. In *Proceedings of the AAAI Conference on Artificial Intelligence*, pages 10680–10687, 2020. 2

[7] Mohammad Reza Karimi Dastjerdi, Jonathan Eisenmann, Yannick Hold-Geoffroy, and Jean-François Lalonde. Everlight: Indoor-outdoor editable hdr lighting estimation. In *Proceedings of the IEEE/CVF international conference on computer vision*, pages 7420–7429, 2023. 3

[8] Bin Ding, Chengjiang Long, Ling Zhang, and Chunxia Xiao. Argan: Attentive recurrent generative adversarial network for shadow detection and removal. In *Proceedings of the IEEE/CVF international conference on computer vision*, pages 10213–10222, 2019. 2

[9] Gareth Funka-Lea and Ruzena Bajcsy. Combining color and geometry for the active, visual recognition of shadows. In *Proceedings of IEEE International Conference on Computer Vision*, pages 203–209. IEEE, 1995. 2

[10] Marc-André Gardner, Yannick Hold-Geoffroy, Kalyan Sunkavalli, Christian Gagné, and Jean-François Lalonde. Deep parametric indoor lighting estimation. In *Proceedings of the IEEE/CVF International Conference on Computer Vision*, pages 7175–7183, 2019. 3

[11] Lanqing Guo, Chong Wang, Wenhan Yang, Siyu Huang, Yufei Wang, Hanspeter Pfister, and Bihan Wen. Shadow-diffusion: When degradation prior meets diffusion model for shadow removal. In *Proceedings of the IEEE/CVF Conference on Computer Vision and Pattern Recognition*, pages 14049–14058, 2023. 2

[12] Ruiqi Guo, Qieyun Dai, and Derek Hoiem. Paired regions for shadow detection and removal. *IEEE transactions on pattern analysis and machine intelligence*, 35(12):2956–2967, 2012. 2

[13] Shilin Hu, Hieu Le, ShahRukh Athar, Sagnik Das, and Dimitris Samaras. Shadow removal refinement via material-consistent shadow edges. *2025 IEEE/CVF Winter Conference on Applications of Computer Vision (WACV)*, pages 2631–2641, 2024. 2

[14] Xiaowei Hu, Lei Zhu, Chi-Wing Fu, Jing Qin, and Pheng-Ann Heng. Direction-aware spatial context features for shadow detection. In *Proceedings of the IEEE conference on computer vision and pattern recognition*, pages 7454–7462, 2018. 2

[15] Xiaowei Hu, Yitong Jiang, Chi-Wing Fu, and Pheng-Ann Heng. Mask-shadowgan: Learning to remove shadows from unpaired data. In *Proceedings of the IEEE/CVF international conference on computer vision*, pages 2472–2481, 2019. 2

[16] Xiaowei Hu, Tianyu Wang, Chi-Wing Fu, Yitong Jiang, Qiong Wang, and Pheng-Ann Heng. Revisiting shadow detection: A new benchmark dataset for complex world. *IEEE Transactions on Image Processing*, 30:1925–1934, 2021. 1, 2, 4, 5, 6, 7

[17] Yeying Jin, Wei Ye, Wenhan Yang, Yuan Yuan, and Robby T Tan. Des3: Adaptive attention-driven self and soft shadow removal using vit similarity. In *Proceedings of the AAAI Conference on Artificial Intelligence*, pages 2634–2642, 2024. 2

[18] Pakorn KaewTraKulPong and Richard Bowden. An improved adaptive background mixture model for real-time tracking with shadow detection. *Video-based surveillance systems: Computer vision and distributed processing*, pages 135–144, 2002. 1

[19] Diederik P. Kingma and Jimmy Ba. Adam: A method for stochastic optimization. In *ICLR*, 2015. 5

[20] Jean-François Lalonde, Alexei A Efros, and Srinivasa G Narasimhan. Detecting ground shadows in outdoor consumer photographs. In *Computer Vision–ECCV 2010: 11th European Conference on Computer Vision, Heraklion, Crete, Greece, September 5–11, 2010, Proceedings, Part II* 11, pages 322–335. Springer, 2010. 1

[21] Hieu Le and Dimitris Samaras. Shadow removal via shadow image decomposition. In *Proceedings of the IEEE/CVF International Conference on Computer Vision*, pages 8578–8587, 2019. 2

[22] Hieu Le and Dimitris Samaras. From shadow segmentation to shadow removal. In *ECCV*, 2020.

[23] Hieu Le and Dimitris Samaras. Physics-based shadow image decomposition for shadow removal. *IEEE Transactions on Pattern Analysis and Machine Intelligence*, 44(12):9088–9101, 2021. 2

[24] Hieu Le, Vu Nguyen, Chen-Ping Yu, and D. Samaras. Geodesic distance histogram feature for video segmentation. *ACCV*, 2016. 2

[25] Hieu Le, Chen-Ping Yu, Gregory Zelinsky, and Dimitris Samaras. Co-localization with category-consistent features

and geodesic distance propagation. In *ICCV 2017 Workshop on CEFRL: Compact and Efficient Feature Representation and Learning in Computer Vision*, 2017. 2

[26] Hieu Le, Tomas F Yago Vicente, Vu Nguyen, Minh Hoai, and Dimitris Samaras. A+ d net: Training a shadow detector with adversarial shadow attenuation. In *Proceedings of the European Conference on Computer Vision (ECCV)*, pages 662–678, 2018. 2

[27] Hieu Le, Bento Goncalves, Dimitris Samaras, and Heather Lynch. Weakly labeling the antarctic: The penguin colony case. In *CVPR Workshops*, 2019. 2

[28] Hieu Le, Dimitris Samaras, and Heather J. Lynch. A convolutional neural network architecture designed for the automated survey of seabird colonies. *Remote Sensing in Ecology and Conservation*, 8(2):251–262, 2022. 2

[29] Xiaoguang Li, Qing Guo, Rabab Abdelfattah, Di Lin, Wei Feng, Ivor Tsang, and Song Wang. Leveraging inpainting for single-image shadow removal. In *Proceedings of the IEEE/CVF International Conference on Computer Vision*, pages 13055–13064, 2023. 2

[30] Zhuang Liu, Hanzi Mao, Chao-Yuan Wu, Christoph Feichtenhofer, Trevor Darrell, and Saining Xie. A convnet for the 2020s. *Proceedings of the IEEE/CVF Conference on Computer Vision and Pattern Recognition (CVPR)*, 2022. 5

[31] Thomas Müller and Bastian Erdnüeß. Brightness correction and shadow removal for video change detection with uavs. In *Autonomous Systems: Sensors, Processing, and Security for Vehicles and Infrastructure 2019*, page 1100906. SPIE, 2019. 1

[32] Takahiro Okabe, Imari Sato, and Yoichi Sato. Attached shadow coding: Estimating surface normals from shadows under unknown reflectance and lighting conditions. In *2009 IEEE 12th International Conference on Computer Vision*, pages 1693–1700. IEEE, 2009. 2

[33] Alexandros Panagopoulos, Dimitris Samaras, and Nikos Paragios. Robust shadow and illumination estimation using a mixture model. In *2009 IEEE Conference on Computer Vision and Pattern Recognition*, pages 651–658. IEEE, 2009. 1

[34] Alexandros Panagopoulos, Tomás F Yago Vicente, and Dimitris Samaras. Illumination estimation from shadow borders. In *2011 IEEE International Conference on Computer Vision Workshops (ICCV Workshops)*, pages 798–805. IEEE, 2011.

[35] Alexandros Panagopoulos, Chaohui Wang, Dimitris Samaras, and Nikos Paragios. Illumination estimation and cast shadow detection through a higher-order graphical model. In *CVPR 2011*, pages 673–680. IEEE, 2011.

[36] Alexandros Panagopoulos, Chaohui Wang, Dimitris Samaras, and Nikos Paragios. Estimating shadows with the bright channel cue. In *Trends and Topics in Computer Vision: ECCV 2010 Workshops, Heraklion, Crete, Greece, September 10-11, 2010, Revised Selected Papers, Part II 11*, pages 1–12. Springer, 2012. 2

[37] Alexandros Panagopoulos, Chaohui Wang, Dimitris Samaras, and Nikos Paragios. Simultaneous cast shadows, illumination and geometry inference using hypergraphs. *IEEE transactions on pattern analysis and machine intelligence*, 35(2):437–449, 2012. 1, 2, 3

[38] Adam Paszke, Sam Gross, Francisco Massa, Adam Lerer, James Bradbury, Gregory Chanan, Trevor Killeen, Zeming Lin, Natalia Gimelshein, Luca Antiga, et al. Pytorch: An imperative style, high-performance deep learning library. *Advances in neural information processing systems*, 32, 2019. 5

[39] Pakkapon Phongthawee, Worameth Chinchuthakun, Non-taphat Sinsunthithet, Varun Jampani, Amit Raj, Pramook Khungurn, and Supasorn Suwajanakorn. Diffusionlight: Light probes for free by painting a chrome ball. In *Proceedings of the IEEE/CVF conference on computer vision and pattern recognition*, pages 98–108, 2024. 3

[40] Liangqiong Qu, Jiandong Tian, Shengfeng He, Yandong Tang, and Rynson WH Lau. Deshadownet: A multi-context embedding deep network for shadow removal. In *Proceedings of the IEEE conference on computer vision and pattern recognition*, pages 4067–4075, 2017. 2

[41] Dimitrios Samaras and Dimitris Metaxas. Incorporating illumination constraints in deformable models for shape from shading and light direction estimation. *IEEE Transactions on Pattern Analysis and Machine Intelligence*, 25(2):247–264, 2003. 2

[42] Imari Sato, Yoichi Sato, and Katsushi Ikeuchi. Illumination from shadows. *IEEE Transactions on Pattern Analysis and Machine Intelligence*, 25(3):290–300, 2003. 2

[43] Gowri Somanath and Daniel Kurz. Hdr environment map estimation for real-time augmented reality. In *Proceedings of the IEEE/CVF conference on computer vision and pattern recognition*, pages 11298–11306, 2021. 3

[44] Jürgen Stander, Roland Mech, and Jörn Ostermann. Detection of moving cast shadows for object segmentation. *IEEE Transactions on multimedia*, 1(1):65–76, 1999. 2

[45] Nan Su, Ye Zhang, Shu Tian, Yiming Yan, and Xinyuan Miao. Shadow detection and removal for occluded object information recovery in urban high-resolution panchromatic satellite images. *IEEE Journal of Selected Topics in Applied Earth Observations and Remote Sensing*, 9:2568–2582, 2016. 1

[46] Carole H Sudre, Wenqi Li, Tom Vercauteren, Sébastien Ourselin, and M Jorge Cardoso. Generalised dice overlap as a deep learning loss function for highly unbalanced segmentations. In *International Workshop on Deep Learning in Medical Image Analysis*, pages 240–248. Springer, 2017. 4

[47] Jiayu Sun, Ke Xu, Youwei Pang, Lihe Zhang, Huchuan Lu, Gerhard Hancke, and Rynson Lau. Adaptive illumination mapping for shadow detection in raw images. In *Proceedings of the IEEE/CVF International Conference on Computer Vision*, pages 12709–12718, 2023. 2

[48] Kalyan Sunkavalli, Todd Zickler, and Hanspeter Pfister. Visibility subspaces: Uncalibrated photometric stereo with shadows. In *Computer Vision–ECCV 2010: 11th European Conference on Computer Vision, Heraklion, Crete, Greece, September 5–11, 2010, Proceedings, Part II 11*, pages 251–264. Springer, 2010. 1

[49] Shailaja Surkutlawar and R. Kulkarni. Shadow suppression using rgb and hsv color space in moving object detection. *International Journal of Advanced Computer Science and Applications*, 4:164–169, 2013. 1

[50] Florin-Alexandru Vasluijanu, Tim Seizinger, Zhuyun Zhou, Zongwei Wu, Cailian Chen, Radu Timofte, Wei Dong, Han Zhou, Yuqiong Tian, Jun Chen, et al. Ntire 2024 image shadow removal challenge report. In *Proceedings of the IEEE/CVF Conference on Computer Vision and Pattern Recognition*, pages 6547–6570, 2024. 2, 4, 5

[51] Dor Verbin, Ben Mildenhall, Peter Hedman, Jonathan T Barron, Todd Zickler, and Pratul P Srinivasan. Eclipse: Disambiguating illumination and materials using unintended shadows. In *Proceedings of the IEEE/CVF Conference on Computer Vision and Pattern Recognition*, pages 77–86, 2024. 3

[52] Tomás F Yago Vicente, Le Hou, Chen-Ping Yu, Minh Hoai, and Dimitris Samaras. Large-scale training of shadow detectors with noisily-annotated shadow examples. In *Computer Vision–ECCV 2016: 14th European Conference, Amsterdam, The Netherlands, October 11–14, 2016, Proceedings, Part VI 14*, pages 816–832. Springer, 2016. 1, 2

[53] Jifeng Wang, Xiang Li, and Jian Yang. Stacked conditional generative adversarial networks for jointly learning shadow detection and shadow removal. In *Proceedings of the IEEE conference on computer vision and pattern recognition*, pages 1788–1797, 2018. 2

[54] Tianyu Wang, Xiaowei Hu, Qiong Wang, Pheng-Ann Heng, and Chi-Wing Fu. Instance shadow detection. In *Proceedings of the IEEE/CVF Conference on Computer Vision and Pattern Recognition*, pages 1880–1889, 2020. 1, 2, 4, 5

[55] Tianyu Wang, Xiaowei Hu, Chi-Wing Fu, and Pheng-Ann Heng. Single-stage instance shadow detection with bidirectional relation learning. In *Proceedings of the IEEE/CVF Conference on Computer Vision and Pattern Recognition*, pages 1–11, 2021.

[56] Tianyu Wang, Xiaowei Hu, Pheng-Ann Heng, and Chi-Wing Fu. Instance shadow detection with a single-stage detector. *IEEE Transactions on Pattern Analysis and Machine Intelligence*, 45(3):3259–3273, 2022. 2

[57] Yifan Wang, Brian L Curless, and Steven M Seitz. People as scene probes. In *Computer Vision–ECCV 2020: 16th European Conference, Glasgow, UK, August 23–28, 2020, Proceedings, Part X 16*, pages 438–454. Springer, 2020. 1

[58] Yonghui Wang, Shaokai Liu, Li Li, Wengang Zhou, and Houqiang Li. Swinshadow: Shifted window for ambiguous adjacent shadow detection. *ACM Transactions on Multimedia Computing, Communications and Applications*, 2024. 2

[59] Haoyu Wu, Jingyi Xu, Hieu Le, and Dimitris Samaras. Importance-based token merging for efficient image and video generation. In *ICCV*, 2025. 2

[60] Jingyi Xu and Hieu Le. Generating representative samples for few-shot classification. In *CVPR*, 2022.

[61] Jingyi Xu, Hieu Le, Mingzhen Huang, ShahRukh Athar, and Dimitris Samaras. Variational feature disentangling for fine-grained few-shot classification. In *ICCV*, 2021.

[62] Jingyi Xu, Hieu Le, Vu Nguyen, Viresh Ranjan, and Dimitris Samaras. Zero-shot object counting. *CVPR*, pages 15548–15557, 2023.

[63] Jingyi Xu, Hieu Le, and Dimitris Samaras. Generating features with increased crop-related diversity for few-shot object detection. In *CVPR*, 2023.

[64] Jingyi Xu, Hieu Le, and Dimitris Samaras. Assessing sample quality via the latent space of generative models. In *ECCV*, 2024. 2

[65] Han Yang, Tianyu Wang, Xiaowei Hu, and Chi-Wing Fu. Silt: Shadow-aware iterative label tuning for learning to detect shadows from noisy labels. In *Proceedings of the IEEE/CVF International Conference on Computer Vision*, pages 12687–12698, 2023. 1, 2, 5, 6, 7

[66] Lihe Yang, Bingyi Kang, Zilong Huang, Zhen Zhao, Xiaogang Xu, Jiashi Feng, and Hengshuang Zhao. Depth anything v2. *arXiv preprint arXiv:2406.09414*, 2024. 2, 5, 8

[67] Jinsong Zhang, Kalyan Sunkavalli, Yannick Hold-Geoffroy, Sunil Hadap, Jonathan Eisenman, and Jean-François Lalonde. All-weather deep outdoor lighting estimation. In *Proceedings of the IEEE/CVF conference on Computer Vision and Pattern Recognition*, pages 10158–10166, 2019. 3

[68] Wuming Zhang, Xi Zhao, Jean-Marie Morvan, and Liming Chen. Improving shadow suppression for illumination robust face recognition. *IEEE Transactions on Pattern Analysis and Machine Intelligence*, 41:611–624, 2019. 1

[69] Peng Zheng, Dehong Gao, Deng-Ping Fan, Li Liu, Jorma Laaksonen, Wanli Ouyang, and Nicu Sebe. Bilateral reference for high-resolution dichotomous image segmentation. *arXiv preprint arXiv:2401.03407*, 2024. 5

[70] Quanlong Zheng, Xiaotian Qiao, Ying Cao, and Rynson WH Lau. Distraction-aware shadow detection. In *Proceedings of the IEEE/CVF conference on computer vision and pattern recognition*, pages 5167–5176, 2019. 2, 5, 7

[71] Lei Zhu, Zijun Deng, Xiaowei Hu, Chi-Wing Fu, Xuemiao Xu, Jing Qin, and Pheng-Ann Heng. Bidirectional feature pyramid network with recurrent attention residual modules for shadow detection. In *Proceedings of the European Conference on Computer Vision (ECCV)*, pages 121–136, 2018. 2, 5, 6, 7

[72] Lei Zhu, Ke Xu, Zhanghan Ke, and Rynson WH Lau. Mitigating intensity bias in shadow detection via feature decomposition and reweighting. In *Proceedings of the IEEE/CVF International Conference on Computer Vision*, pages 4702–4711, 2021. 2, 5, 6, 7

[73] Yurui Zhu, Xueyang Fu, Chengzhi Cao, Xi Wang, Qibin Sun, and Zheng-Jun Zha. Single image shadow detection via complementary mechanism. In *Proceedings of the 30th ACM International Conference on Multimedia*, pages 6717–6726, 2022. 1, 2, 5, 7

[74] Zhe Zhu and Curtis E Woodcock. Object-based cloud and cloud shadow detection in landsat imagery. *Remote sensing of environment*, 118:83–94, 2012. 1